

# Design and Analysis of a 150 K Cascade Joule-Thomson Microcooler

R. Radebaugh<sup>1</sup>, P. Bradley<sup>1</sup>, C. Coolidge<sup>2</sup>, R. Lewis<sup>2</sup>, and Y.C. Lee<sup>2</sup>

<sup>1</sup>National Institute of Standards and Technology, Boulder, CO 80305 USA

<sup>2</sup>University of Colorado, Boulder, CO 80309 USA

## ABSTRACT

Lightweight and compact microcoolers are needed for advanced, hand-held infrared systems. A temperature of 150 K is adequate for high sensitivity with some of the latest IR detectors, which simplifies the cooling requirements compared to 80 K detectors. The largest and heaviest component of most gas-cycle cryocoolers has been the compressor. This paper describes how the use of a 150 K, five-stage, cascade Joule-Thomson (JT) cycle significantly reduces the total refrigerant flow rate and total compressor swept volume compared with other types of cryocoolers for this temperature range. The use of vapor compression in each of the five stages results in very high specific refrigeration powers and low flow rates even with no recuperative heat exchangers and with pressure ratios of only about 4:1. Such low pressure ratios are needed for the use of chip-scale compressors. We discuss the thermodynamic design of a five-stage planar polyimide cold head for a range of refrigeration powers up to about 350 mW at 150 K. We compare the use of single-layer and double-layer construction over this range of refrigeration powers. In the double-layer construction, the high-pressure fluid streams are on the bottom and the low-pressure fluid streams are on top. Such construction allows for simple recuperative heat exchangers and leads to a compact planar geometry of about 20 mm by 30 mm for 350 mW refrigeration power at 150 K. The ideal fluid input power for the five-stage system at 150 K with no recuperative heat exchangers is 1.59 W per watt of net refrigeration power. For a heat exchanger ineffectiveness of 0.05 the specific power is 1.29 W/W for an efficiency of 89.2 % of Carnot with perfect compressors. The paper describes the geometry of the condensers, evaporators and Joule-Thomson impedances to achieve the high heat flux required for minimum size.

## INTRODUCTION

Temperatures around 150 K are required for many of the new high-performance infrared sensors. Refrigeration powers can vary from about 0.1 W to 0.5 W depending on the size of the focal plane array. These sensors are becoming much smaller than the existing cryocoolers available to cool them. To enable the use of these sensors in such applications as human-portable devices, unattended aerial vehicles, and micro-satellites, it is important to shrink the size of the cryocooler and reduce its mass to something comparable to that of the sensor. It is also important to maintain a high efficiency so that the motor and battery size required for supplying power to the cryocooler can be kept very compact and last for a long time period between

charges. Generally, the compressor is the largest item in a cryocooler, and it is especially true in the current development of microcryocoolers. Thus, to reduce the size of cryocoolers, we must pay close attention to what is required to reduce the compressor size. We first look at previous microcryocooler efforts to understand the state of the art and to learn where additional effort is required to reduce their size further, improve their efficiency, and modify them in a way to reduce cost through common mass-production techniques, such as wafer-level fabrication.

Previous work on Joule-Thomson (JT) microcryocoolers<sup>1-6</sup>, which was reviewed by Radebaugh<sup>7</sup>, used either compressed cylinders of gas or relatively large sorption compressors to feed a micro-coldhead. Inlet pressures were usually greater than 8 MPa and pressure ratios were usually greater than 80:1. The development of microcompressors is currently at its infancy, and such high pressures and pressure ratios are not feasible with them anytime soon. With that limitation in mind, a program at the University of Colorado and NIST/Boulder (CU/NIST) funded by DARPA focused on the use of mixed refrigerants in micro cryogenic coolers (MCCs). Optimized mixed refrigerants were found that could provide nearly an order of magnitude higher specific cooling powers (refrigeration per unit flow) compared with pure refrigerants for temperatures of 150 K for pressure ratios as small as 4:1<sup>8,9</sup>.

This same CU/NIST program also led to the development of a planar polyimide cold head, as shown in Fig. 1, for refrigeration powers of about 10 mW at 200 K<sup>10</sup>. Polyimide has about an order of magnitude lower thermal conductivity than that of glass, which allows for shorter coldheads and a reduction in the surface area exposed to room-temperature radiation. In scaling to small sizes, radiation heat leak becomes a dominate source of loss because of the increase in surface to volume ratio. Figure 2 shows the cool down behavior of a monolithic polyimide coldhead<sup>11</sup> when it was driven with a rotary Stirling compressor modified with the addition of inlet and outlet valves<sup>12</sup>. The compressor was orders of magnitude larger than the cold head, but the project demonstrated that inlet and outlet valves for pressure ratios up to 6:1 could be successfully micro-fabricated with polyimide. The presence of the temperature pulsations, as shown in Fig. 2 for the polyimide cold head and also seen earlier in glass capillary coldheads<sup>8</sup>, is a disadvantage of using mixed refrigerants in microscale geometries. Lewis et al.<sup>13</sup> has shown that the flow and temperature pulsations are a result of liquid slugs passing through the cold head that had built up in much larger void volumes between the compressor and the cold head. The liquid consisted mostly of the high boiling-point component. Ideally a two-phase flow should occur throughout most of the cold head. The deviation from ideal flow results in a significant reduction of the refrigeration power compared with the bulk thermodynamic value<sup>13</sup>.

A reduction in cryocooler size is brought about by the following criteria: (1) higher specific refrigeration power, (2) higher heat transfer coefficient between fluid and structure, (3) lower cold head thermal conductivity, and (4) higher compressor frequency. We consider only the first three criteria here. Unlike regenerative cryocoolers, such as Stirling and pulse tube cryocoolers,

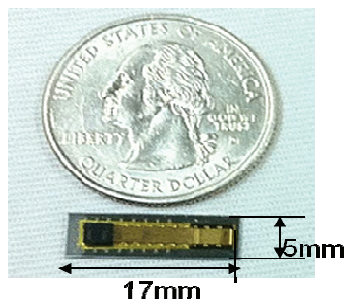


**Figure 1.** Planar polyimide cold head for use with mixed refrigerants at 200 K<sup>10</sup>.

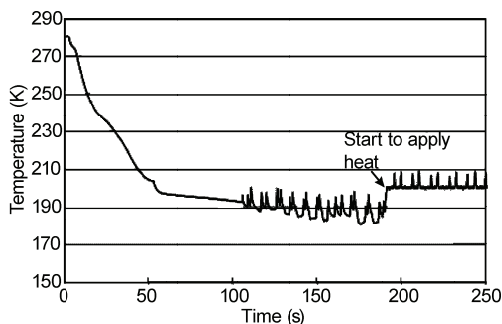


**Figure 2.** Cooldown behavior of polyimide cold head using mixed refrigerant optimized for 200 K showing temperature pulsations<sup>11</sup>.

the compressor frequency can be made very high for JT coolers to reduce the required compressor swept volume for a given flow. The gross refrigeration power of the Joule-Thomson cycle is given by<sup>14</sup>:

$$\dot{Q}_r = \dot{n}(\Delta h_T)_{\min}, \quad (1)$$

where  $\dot{n}$  is the molar flow rate and  $(\Delta h_T)_{\min}$  is the minimum isothermal enthalpy difference between the high- and low-pressure streams over the temperature span between the low and high temperature. In Eq. (1) the parameter  $(\Delta h_T)_{\min}$  is the specific refrigeration power. When losses, such as conduction, radiation, and heat exchanger ineffectiveness are subtracted from the gross refrigeration power, the result is the net refrigeration power  $\dot{Q}_{net}$ . To achieve a low flow and low compressor input power, the specific refrigeration power  $(\Delta h_T)_{\min}$  should be as high as possible for a given refrigeration power. The low flow leads to both a smaller compressor and a smaller cold head. In this paper we examine the use of the vapor-compression cycle in a cascade arrangement to reach 150 K when using a pressure ratio of about 4:1 in all stages.

The use of gaps less than about 50  $\mu\text{m}$  in the evaporators and condensers has the potential of increasing the heat transfer coefficient compared with macroscopic flow channels, although experimental data in such small microchannels is limited. Lower coldhead thermal conductivity and higher heat transfer coefficients have a direct effect on reducing the coldhead size, but because the smaller size reduces radiation heat loss, the compressor flow rate can be reduced as well. The coldhead design given here uses polyimide, which has nearly an order of magnitude lower thermal conductivity than glass. In this paper we consider the specific case of a JT cooler providing 350 mW of net refrigeration at 150 K for the cooling of an infrared focal plane array of about 1  $\text{cm}^2$ .

## THE CASCADE VAPOR-COMPRESSION CYCLE

### Fluids

In the vapor-compression cycle a vapor is condensed at high pressure and high temperature (usually at ambient temperature). The liquid is then expanded isenthalpically through a flow impedance to a low pressure (usually 0.1 MPa) to achieve a low temperature (usually the normal boiling point). Such an isenthalpic expansion is rather efficient because it takes place below the critical point. The cycle does not require a recuperative heat exchanger to reach the low temperature because of the relatively small temperature reduction compared with the normal cryogenic JT cycle. However, a recuperative heat exchanger will increase its efficiency. Figure 3 shows the specific enthalpy of R14 (tetrafluoromethane) as a function of temperature for several pressures. Its normal boiling point of 145 K makes it a good candidate refrigerant for 150 K refrigeration. A pressure of 0.4 MPa is sufficient to condense the vapor at 169 K and greatly reduce its enthalpy. An isenthalpic expansion of the liquid from 169 K to 0.1 MPa and 145 K causes 16 % of the liquid to vaporize, but only 16 % of the available latent heat is sacrificed to reduce the temperature. The remaining 84 % of the latent heat is available for refrigeration at 145 K. Use of a recuperative heat exchanger would allow 92 % of the latent heat to be utilized. Shown for comparison in Fig. 3 is the specific enthalpy of a five-component mixture designed for refrigeration between 140 K and 300 K with a pressure ratio of 4:1. Isenthalpic expansion of the fluid from 0.4 MPa at 300 K to 0.1 MPa only reduces the temperature to about 275 K. Clearly, a recuperative heat exchanger is required to reach 150 K with this mixed refrigerant JT process. As Fig. 3 shows, the isothermal enthalpy change between the high and low pressures for the mixed refrigerant is much less than that of R14 in its two-phase region. However, R14 must be precooled to 169 K by higher temperature stages to be able to condense the vapor at 0.4 MPa. The enthalpy change above the critical temperature and especially at 300 K is very small.

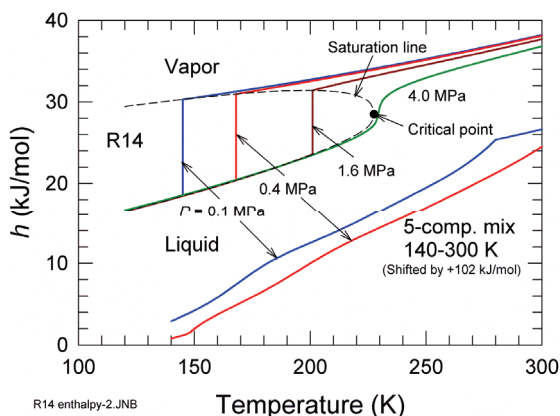


**Figure 3.** Enthalpy of R14, which shows large enthalpy changes during condensation and evaporation. The enthalpy of a five-component mixture is shown for comparison.

Figure 4 shows the isothermal enthalpy change for candidate pure fluids for various stages in a cascade vapor-compression cycle in which the pressure ratio is kept close to 4:1. Only the third stage (R116, hexafluorethane) requires a slightly higher pressure of 0.5 MPa to be condensed at the normal boiling point of propane (231 K). The minimum isothermal enthalpy change ( $\Delta h_T$ )<sub>min</sub> used in Eq. (1) for the temperature range of their use occurs at the condensing temperature for all the pure fluids. Shown for comparison in Fig. 4 is the isothermal enthalpy change of the five component mixed refrigerant designed to maximize ( $\Delta h_T$ )<sub>min</sub> for a 4:1 pressure ratio over the temperature range of 140 K to 300 K<sup>13</sup>. The pure refrigerants operating in the two-phase region have five to ten times higher ( $\Delta h_T$ )<sub>min</sub> than that of the mixed refrigerant, which means the flow in each stage is five to ten times smaller than that of the single mixed-refrigerant compressor, but five separate compressors are required for the cascade approach. Such an approach with five separate compressors only makes sense if it is feasible to mass fabricate chip-scale compressors using wafer-level techniques.

### Layout Schematic

A schematic of a five-stage cascade cycle is shown in Fig. 5. The layout in this schematic is for a single fluid layer and represents the simplest fabrication method. Two types of heat

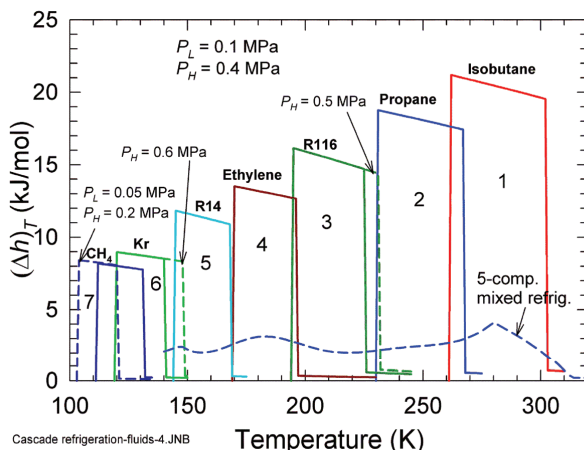


**Figure 4.** Isothermal enthalpy difference between high and low pressures for candidate cascade refrigerants compared with that for a five component mixture.

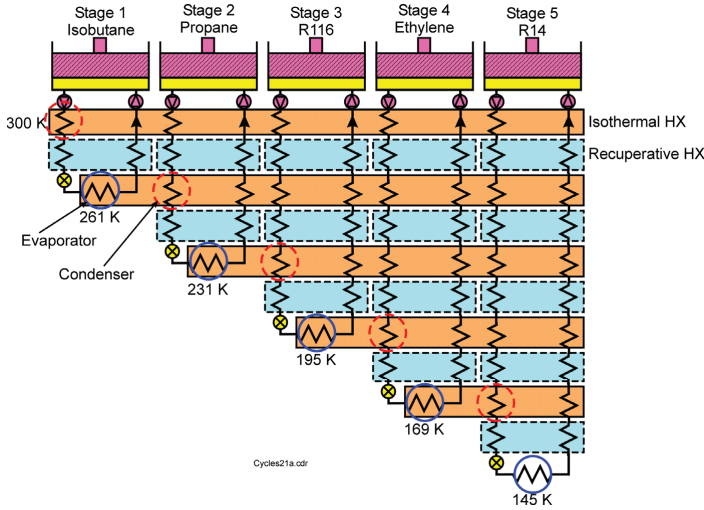


**Figure 5.** Schematic of a five-stage cascade cooler for 145 K showing isothermal and recuperative heat exchangers. Majority of heat transfer is between condensers and evaporators.

exchangers are shown. The recuperative heat exchangers span a significant temperature difference and must be made of low conductivity material, such as polyimide. They need only to exchange heat within any given stage. As discussed earlier, they are not required if isothermal heat exchangers are used at each stage, but they do increase efficiency. The isothermal heat exchangers maintain a uniform temperature and must transport heat to the evaporators of each stage from intercepts in following stages. Most of the transported heat comes from the enthalpy change in the condenser in the following stage, as indicated by the large enthalpy change in Fig. 3 for R14 at 0.4 MPa and 169 K. The sum of all the heat that must be intercepted from R14 by the first three stages in precooling it is the change in enthalpy from 300 K to 195 K, which is somewhat less than the heat flow from the condenser at 169 K. The isothermal heat exchangers must be made with high thermal conductivity material to transport heat some distance. As the number of stages increases, the heat transport distance increases. The transport distance also increases with refrigeration power because the width of flow channels in each stage increases. An upper limit of about 0.5 W of refrigeration at 150 K may occur from our calculations for this planar single-layer construction because of an excessive temperature gradient in the isothermal heat exchangers. In addition to transporting the heat of condensation, the isothermal heat exchangers intercept losses from the recuperative heat exchangers and improve efficiency. Those losses are relatively small unless no recuperative heat exchangers are used.

**Thermodynamic Analysis**

The goal of the DARPA-funded program is to provide 350 mW of net refrigeration power at 150 K. We assumed a gross refrigeration power of 360 mW to take into account reasonable conduction, radiation, and heat exchanger losses to the 150 K stage. Conduction and heat exchanger losses are quite low because of the small 19 K delta T between the next higher stage and the 150 K stage. Using the analysis technique discussed in Ref. 7, the heat loads, flow rates, and ideal isothermal input powers for each of the stages were calculated. The results are shown in Table 1 for the case where no recuperative heat exchangers are used (ineffectiveness  $\lambda = 1.0$ ). Table 2 shows the same data for the case where the heat exchangers ineffectiveness is 0.05. Table 3 gives the results with  $\lambda = 0$ . The results in all three tables assume perfect isothermal heat exchangers, except for the last column. The ideal isothermal input power is calculated by

$$\dot{W}_i = \dot{n}\Delta g_0, \tag{2}$$

**Table 1.** Parameters of cascade and mixed-refrigerant coolers with recuperative ineffectiveness of 1.0.

Stage	Temp. (K)	Fluid	Heat load (W)	$(\Delta h_T)_{\min}$ (kJ/mol)	Molar flow ( $\mu\text{mol/s}$ )	Ideal comp. power (W)	Efficiency % Carnot	$\lambda_{\max}$ $T_{c,i-1}$	$\lambda_{\max}$ 300 K
1	261	Isobutane	482	19.54	30.4	0.0937		5.33	5.33
2	231	Propane	383	17.42	24.8	0.0828		8.86	3.67
3	195	R116	404	14.38	36.1	0.1410		4.52	1.43
4	169	Ethylene	366	12.66	31.2	0.1066		13.55	2.51
5	145	R14	360	10.89	36.5	0.1316		10.70	1.38
Total						0.5558	72.4		
		Mixed	-	2.01	-	-	0		0.0846

**Table 2.** Parameters of cascade and mixed-refrigerant coolers with recuperator ineffectiveness of 0.05.

Stage	Temp. (K)	Fluid	Heat load (W)	$(\Delta h_T)_{\min}$ (kJ/mol)	Molar flow ( $\mu\text{mol/s}$ )	Ideal comp. power (W)	Efficiency % Carnot	$\lambda_{\max}$ $T_{c,i-1}$	$\lambda_{\max}$ 300 K
1	261	Isobutane	384	19.54	19.9	0.0613		5.33	5.33
2	231	Propane	368	17.42	21.2	0.0708		8.86	3.67
3	195	R116	371	14.38	25.9	0.1015		4.52	1.43
4	169	Ethylene	361	12.66	28.6	0.0977		13.55	2.51
5	145	R14	360	10.89	33.2	0.1199		10.70	1.38
Total						0.4512	89.2		
		Mixed	650	2.01	323.4	1.082	34.5		0.0846

**Table 3.** Parameters of cascade and mixed-refrigerant coolers with recuperator ineffectiveness of 0.

Stage	Temp. (K)	Fluid	Heat load (W)	$(\Delta h_T)_{\min}$ (kJ/mol)	Molar flow ( $\mu\text{mol/s}$ )	Ideal comp. power (W)	Efficiency % Carnot	$\lambda_{\max}$ $T_{c,i-1}$	$\lambda_{\max}$ 300 K
1	261	Isobutane	379	19.54	19.4	0.0599		5.33	5.33
2	231	Propane	367	17.42	21.1	0.0703		8.86	3.67
3	195	R116	367	14.38	25.5	0.0999		4.52	1.43
4	169	Ethylene	361	12.66	28.5	0.0973		13.55	2.51
5	145	R14	360	10.89	33.1	0.1193		10.70	1.38
Total						0.4467	90.1		
		Mixed	400	2.01	199.0	0.666	56.2		0.0846

where  $\Delta g_0$  is the change in Gibbs free energy between the low and high pressure at 300 K for each of the fluids. The total ideal input power is the sum of the ideal input powers for each stage. For the case of 0.05 ineffectiveness heat exchangers (Table 2), the ideal input power is 0.451 W or 1.29 W/W of specific power and 89.2% of Carnot efficiency. Even though kilowatt-size compressors may achieve isothermal efficiencies around 50%, we expect microcompressors to have efficiencies more in the range of 9 % early in their development.

We then compare this thermodynamic performance with that of a calculated mixed-refrigerant JT cooler using the optimized five-component refrigerant discussed earlier for the temperature range of 140 K to 300 K. In such a comparison we make use of the maximum heat exchanger ineffectiveness, given by

$$\lambda_{\max} = \frac{(\Delta h_T)_{\max}}{(h_h - h_c)_{\min}}, \quad (3)$$

where  $(h_h - h_c)_{\min}$  is the minimum enthalpy difference between the hot and cold temperature. The last column in Tables 1-3 gives the maximum ineffectiveness for the case where the heat exchanger is precooling from 300 K instead of from the previous stage. The maximum ineffectiveness is that value of ineffectiveness that causes the heat exchanger loss to be equal to the gross refrigeration power. For any higher value it would not be possible to even reach the low temperature. All the stages of the cascade vapor-compression cycle have  $\lambda_{\max}$  considerably greater than 1, which means no recuperative heat exchangers are required in any of the stages to reach the low temperature. As the last column indicates, the cascade cycle even works with no

recuperative heat exchanger and no precooling of any stage below 300 K except for the condensation by the previous stage. However, some form of precooling is needed to maintain high efficiency. For the mixed-refrigerant JT cycle using the five-component mix,  $\lambda_{max} = 0.085$ . Thus, even with a recuperator ineffectiveness of 0.1, the mixed refrigerant cycle will not operate. For an ineffectiveness of 0.05 the heat exchanger loss is  $0.05/0.085 = 0.59$  times the gross refrigeration power. For a net refrigeration power of 0.35 W, the gross refrigeration power must then be at least  $0.35/0.59 = 0.59$  W. Conduction and radiation losses would then require at least 0.65 W of gross refrigeration power. The ideal input power is then 1.082 W for an efficiency of 34.5 % of Carnot. It is this low  $\lambda_{max}$  of the mixed refrigerant compared to that for the cascade cycle that leads to the high input power to overcome the heat exchanger loss.

**COLDHEAD LAYOUT OPTIONS**

**Thermal Resistances in Single- and Double-Layer Coldheads**

The heat flow from one stage to the next and from detector to the last-stage evaporator passes through several thermal resistances. The geometry and layout options chosen for the stages must be made with a goal of minimizing these thermal resistances to maintain high overall efficiency. The effect of excessive temperature drops between stages results in the use of higher pressure ratios and greater input power for the various stages to provide for a greater temperature overlap. The fluids selected here and shown in Fig. 4 have a few degrees of overlap at a pressure ratio of 4:1 except for the R116 stage that requires a high pressure of 0.5 MPa to overlap with propane.

We consider two layout options. A single layer in which all fluid channels are in the same plane leads to the simplest fabrication. The layout would be similar to the schematic shown in Fig. 5. However, the width of the coldhead can become large with this arrangement, which can lead to significant temperature differences between the stages due to excessive thermal resistance in the isothermal heat exchangers. The second layout option is the double layer approach in which the high-pressure streams are on one plane and the low-pressure streams are on another plane. This option permits good heat transfer between the condenser of one stage and the evaporator of the adjacent stage because one can be on top of the other with only a thin polyimide layer (10  $\mu\text{m}$ ) between them.

Figure 6 illustrates the path heat must take in a single-layer coldhead to travel from the condenser of one stage to the evaporator of the preceding stage. The outside polyimide walls are assumed to be 20  $\mu\text{m}$  thick, which is sufficient to contain the 0.4 MPa high pressure.<sup>11</sup> The five thermal resistances are: (1) interface resistance between condensing fluid and polyimide wall, (2) thermal resistance through 20  $\mu\text{m}$  thick polyimide, (3) thermal resistance through copper isothermal strip to preceding stage, (4) thermal resistance through 20  $\mu\text{m}$  thick polyimide, and (5) interface resistance between polyimide and evaporating fluid. For illustration purposes, we consider the case of heat transfer from condensing propane (2<sup>nd</sup> stage) at 0.4 MPa to evaporating isobutane (1<sup>st</sup> stage) at 0.1 MPa. In these calculations, we assume a heat transfer coefficient of 1.0 W/(cm<sup>2</sup>·K) for both the boiling and condensing heat transfer, but there is little data available

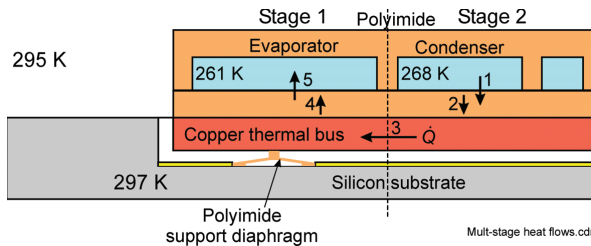


**Figure 6.** Heat flow path from condenser of Stage 2 to evaporator of Stage 1 with the heat passing through five thermal resistances for the case of a single fluid layer.

for two-phase heat transfer in microchannels with gaps less than  $100\ \mu\text{m}$ <sup>15</sup>. The smaller gaps may lead to higher heat transfer coefficients. Further work is needed in this area. As shown in Tables 1 to 3, the heat transfer to the isobutane stage is about  $0.4\ \text{W}$  for the case of a cooler providing  $360\ \text{mW}$  at  $150\ \text{K}$ . For a surface area of  $0.4\ \text{cm}^2$  the  $\Delta T$  for both resistance (1) and (5) is then  $1.0\ \text{K}$  at each surface. The thermal conductivity of polyimide at  $261\ \text{K}$  is about  $0.185\ \text{W}/(\text{m}\cdot\text{K})$ <sup>16</sup>. The  $\Delta T$  through a  $0.4\ \text{cm}^2$  polyimide layer  $20\ \mu\text{m}$  thick is then  $1.1\ \text{K}$ . With a copper strip  $0.4\ \text{mm}$  thick and  $5\ \text{mm}$  wide overlaying the isobutane and propane stages,  $\Delta T = 4.2\ \text{K}$  for a length of  $8\ \text{mm}$ . The total  $\Delta T$  between the stages for this single-layer coldhead is then  $8.4\ \text{K}$ . Half of the  $\Delta T$  is due to the isothermal copper strip, which must be relatively long when high heat loads occur because the surface area of each stage must be sufficiently large to keep the other thermal resistances small. Thus, a single layer coldhead is not a good choice for refrigeration powers much larger than about  $0.2\ \text{W}$  at  $150\ \text{K}$ . For smaller powers, it can be a good choice and simple to fabricate.

With a double-layer coldhead the only thermal resistance between the condenser and the evaporator are resistances (1) and (5) given above and the resistance through a thinner  $10\ \mu\text{m}$  thick polyimide layer separating the two streams<sup>11</sup>. The total temperature drop between stages is then  $\Delta T = 2.6\ \text{K}$ . We then consider the layout for a double-layer coldhead for a  $150\ \text{K}$  cooler.

### Layout for a Double-Layer Coldhead

Figure 7 shows a section of a preliminary layout for a five-stage, double-layer coldhead for a net refrigeration power of  $350\ \text{mW}$  at  $150\ \text{K}$ . In this drawing the high pressure streams are on the bottom and the low pressure streams are on the top. The two layers allow for a good recuperative heat exchanger between the high- and low-pressure streams in each stage. In the case shown here no isothermal heat exchangers are used except for that between the evaporator and condenser of adjacent stages, which is where heat must flow between stages. With no isothermal heat exchangers intercepting heat from the incoming high-pressure stream, some recuperative heat exchange becomes fairly important, especially the lower stages. The last column in Tables 1 to 3 gives the maximum ineffectiveness for these heat exchangers operating between  $300\ \text{K}$  and the evaporator temperature of each stage. We see that for the last stage (R14)  $\lambda_{\text{max}} = 1.38$ , which means that with no recuperative heat exchanger ( $\lambda = 1$ ) all but  $38\%$  of

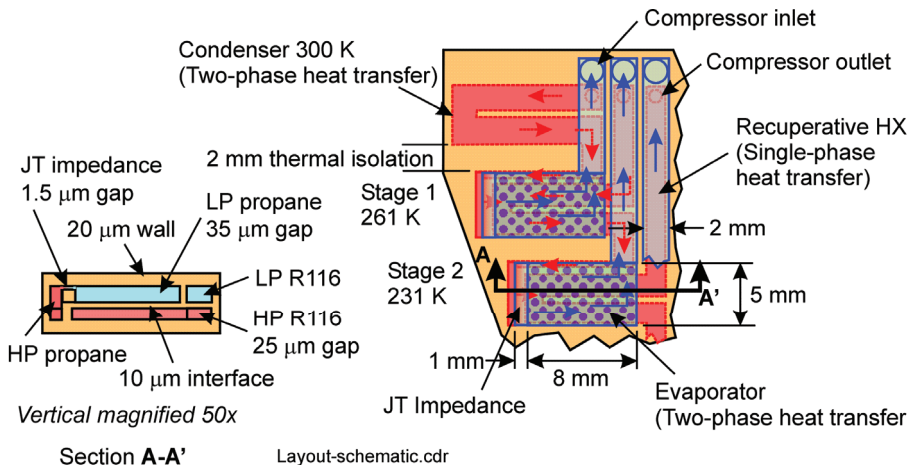


**Figure 7.** Preliminary layout of the coldhead for a double-layer, five-stage cascade cooler for providing  $350\ \text{mW}$  of net refrigeration at  $150\ \text{K}$ . Low-pressure channels are shown on top and high-pressure channels are shown underneath. Overall size for five-stage coldhead is slightly larger than  $20\ \text{mm} \times 30\ \text{mm}$ .



the gross refrigeration power is lost to heat exchanger losses. However, if perfect isothermal heat exchangers are used, then  $\lambda_{\max} = 10.70$  (from second-to-last column in tables) and only about 10 % of the gross refrigeration power is lost if no recuperative heat exchangers are used ( $\lambda = 1$ ;  $\lambda/\lambda_{\max} = 0.093$ ). In our case with no isothermal heat exchangers, we use a reasonable design goal for the ineffectiveness of each recuperative heat exchanger to be less than about 10 % of the maximum listed in the last column of the tables.

The gap thickness of all flow channels must be sufficiently large to keep the pressure drop less than about 5 % of the pressure, except for the JT impedance. However, the heat exchanger ineffectiveness increases with gap thickness, so a compromise is required. For laminar flow in rectangular channels with width  $w$  much greater than the thickness  $t_g$ , the pressure drop is given by

$$\Delta P = \frac{12\dot{n}\mu L}{D_m w t_g^3}, \tag{4}$$

where  $\dot{n}$  is the molar flow rate,  $\mu$  is the viscosity,  $L$  is the length, and  $D_m$  is the molar density. The effect of the pressure drop is to either increase the power input to the compressor for the same refrigeration power or to reduce the refrigeration power for the same power input. The power input for an ideal gas is given by

$$\dot{W} = R_0 T_0 \ln P_r, \tag{5}$$

where  $R_0$  is the molar gas constant,  $T_0$  is the ambient temperature, and  $P_r$  is the pressure ratio. A relative pressure drop leads to a relative increase of input power (or reduction of refrigeration) given by

$$\frac{\Delta \dot{W}}{\dot{W}} = \frac{1}{\ln P_r} \frac{\Delta P}{P}. \tag{6}$$

The number of heat transfer units  $N_{tu}$  for laminar flow along one side of the gap heat exchanger is given by

$$N_{tu} = \frac{8.5\mu w L}{M \dot{n} N_{Pr}^{2/3} t_g}, \tag{7}$$

where  $M$  is the molar mass, and  $N_{Pr}$  is the Prandtl number. The ineffectiveness of the heat exchanger is then given by

$$\lambda = \frac{1}{1 + (N_{tu} / 2)}. \tag{8}$$

The relative loss of refrigeration power caused by the ineffectiveness is given by

$$\Delta \dot{Q}_r / \dot{Q}_r = \lambda / \lambda_{\max}. \tag{9}$$

The relative losses associated with the pressure drop and the heat exchanger ineffectiveness on the low-pressure side are shown in Fig. 8 for the isobutane stage as a function of the gap thickness for a width of 2 mm and a length of 5 mm. We see that the sum of the losses is minimized for a gap thickness of about 40  $\mu\text{m}$ , although gaps as small as 25  $\mu\text{m}$  increase the total loss only slightly. For the same gap on the high-pressure side, the relative loss due to pressure drop is significantly lower because of the much higher density of the liquid. The gap for the high-pressure side can be decreased to about 25  $\mu\text{m}$  without a significant loss in pressure. For the case of the R14 stage the total heat exchanger length is about 37 mm. The gap thickness must then be increased to about 55  $\mu\text{m}$  on the low-pressure side and about 40  $\mu\text{m}$  on the high-pressure side to minimize the losses for that stage.

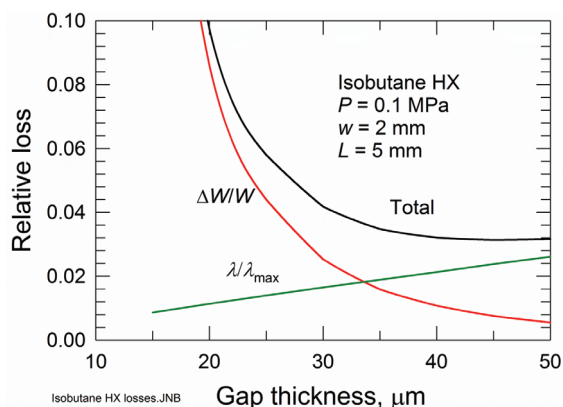


**Figure 8.** Relative losses in the recuperative heat exchanger for isobutane as a function of gap thickness.  $\Delta W/W$  is the relative increase of input power or relative loss in refrigeration due to pressure drop and  $\lambda/\lambda_{\max}$  is the relative loss in refrigeration due to heat exchanger ineffectiveness.

### JOULE-THOMSON IMPEDANCE

The desired flow rate for each stage to give the required refrigeration power is determined from Eq. (1) and listed in Tables 1 to 3. For a given high pressure  $P_H$  and a low pressure  $P_L$ , the flow rate through a gap is given by the integral form of Eq. (4) as

$$\dot{n} = \frac{w_l^3 P_H}{12L} \int_{P_L}^{P_H} \frac{D_m}{\mu} dP. \quad (10)$$

The temperature used for evaluating the density and viscosity depends on whether the expansion is isothermal or isenthalpic. An isothermal expansion occurs if the incoming high pressure fluid is precooled by the returning cold vapor and the evaporation in the evaporator. That is the case for the layout shown in Fig. 7. The high-pressure stream flows below the evaporator before reaching the JT impedance. The width of the JT impedance in this layout is 5 mm and the length is 1 mm. Equation (10) is easily evaluated in this isothermal case for the gap thickness to provide the desired flow. The gap thickness  $t_g$  for the isobutane stage is found to be  $1.53 \mu\text{m}$  for a flow of  $20.3 \mu\text{mol/s}$  ( $\lambda = 0.1$ ). A gap of  $1.00 \mu\text{m}$  would reduce the flow to  $5.63 \mu\text{mol/s}$  and provide 110 mW of gross refrigeration (about 100 mW net) at the isobutane 261 K stage. Thus, the gap thickness must be controlled rather accurately because of the  $t_g^3$  in Eq. (10). If the high-pressure liquid does not exchange heat after the condenser with the returning vapor, the expansion is isenthalpic and the resulting temperature as a function of pressure must be determined in order to evaluate the properties in the integral of Eq. (10). In that case the gap thickness needs to be decreased to about 96 % of that for the isothermal case to account for the lower viscosity of the liquid at higher temperatures.

### CONCLUSIONS

A cascade cycle using five vapor-compression stages to reach 150 K using a pressure ratio of only about 4:1 has been analyzed for use in a microcooler using a planar polyimide coldhead. A thermodynamic analysis showed that the overall efficiency of the system with perfect compressors and with 0.05 ineffectiveness recuperative heat exchangers is 89.2% of Carnot compared to 34.5% of Carnot for a single-stage, mixed-refrigerant cooler for the same temperature range and with 0.05 heat exchanger ineffectiveness. The use of five stages greatly relaxes the heat exchanger requirements for the cascade cycle. Both a single fluid-layer system

and a double fluid-layer system were analyzed for a coldhead providing 350 mW of net refrigeration at 150 K. We showed that for refrigeration powers greater than about 200 mW the thermal resistance in a copper isothermal strip connecting the stages becomes too large for an efficient system, but it could be considered for refrigeration powers up to about 500 mW. A preliminary layout of a double-layer system was presented in which the high- and low-pressure streams are on different planes. The double-layer system leads to simple and effective recuperative heat exchangers, which alleviates the need for isothermal heat exchangers between stages except between the condenser and evaporator of adjacent stages. The overall size of the coldhead is slightly larger than 20 mm by 30 mm but could be reduced with further refinements. The size is dominated by the required surface area for the two-phase heat transfer in the condensers and evaporators based on published experiments with gaps larger than about 100  $\mu\text{m}$ . In our case the gaps are less than about 50  $\mu\text{m}$ , which may lead to higher heat transfer coefficients for two-phase flow. Further research is needed on heat transfer coefficients in two-phase flow for both condensation and evaporation with low-temperature refrigerants. The coldhead presented here is much smaller than existing coolers for refrigeration powers of about 350 mW. The coldhead described here is to be driven with high-frequency, chip-scale microcompressors, which are currently under development as part of this program on micro cryogenic coolers.

## ACKNOWLEDGMENT

Funding for this work was provided by the Micro Cryogenic Cooler (MCC) program of the DARPA Microsystems Technology Office with Dr. Nibir Dhar followed by Dr. Dev Palmer as the program managers. The U.S. Army Research Laboratory (ARL) Cooperative Agreement representative was Dr. Ronald Polcawich.

## REFERENCES

1. Garvey, S., Logan, S., Rowe, R., and Little, W. A., "Performance characteristics of a low flow rate 25 mW,  $\text{LN}_2$  Joule-Thomson refrigerator fabricated by photolithographic means," *Appl. Phys. Letters* **42**, pp. 1048-1050 (1983).
2. Holland, H.J., Burger, J.F., Boersma, N., ter Brake, H.J.M., and Rogalla, H., "Miniature 10-150 mW Linde-Hampson cooler with glass-tube heat exchanger operating with nitrogen," *Cryogenics* **38** (1998), pp. 407-410.
3. Burger, J., Holland, H., Seppenwoodle, J., Berenschot, E., ter Brake, H., Gardeniers, J., Elwenspoek, M., and Rogalla, H., "165 K Microcooler Operating with a Sorption Compressor and Micromachined Cold Stage," *Cryocoolers 11*, Kluwer Academic/Plenum Publishers, New York (2001), pp. 551-560.
4. Lerou, P.P.P.M., ter Brake, H.J.M., Jansen, H.V., Burger, J.F., Holland, H.J., and Rogalla, H., "Micromachined Joule-Thomson Coolers," *Adv. in Cryogenic Engineering*, Vol. 53, Amer. Institute of Physics, Melville, NY (2008), pp. 614-621.
5. Lerou, P.P.P.M., Venborst, G.C.F., Berends, C.F., Veenstra, T.T., Blorn, M., Burger, J.F., ter Brake, H.J.M., and Rogalla, H., "Fabrication of a micro cryogenic cold stage using MEMS technology," *J. Micromechanics and Micromachining* **16**, pp. 1919-1925 (2006).
6. Cao, H.S., Holland, H.J., Vermeer, C.H., Vanapalli, S., Lerou, P.P.P.M., Blom, M., and ter Brake, H.J.M., "Micromachined cryogenic cooler for cooling electronic devices down to 30 K," *J. Micromech. Microeng.* **23**, 025014 (2013).
7. Radebaugh, R., "Thermodynamic Analysis of Cascade Microcryocoolers with Low Pressure Ratios," *Adv. in Cryogenic Engineering*, Vol. 59, Amer. Institute of Physics, Melville, NY (2014), pp. 132-141.
8. Lin, M.-H., Bradley, P.E., Huber, M.L., Lewis, R., Radebaugh, R., and Lee, Y.C., "Mixed refrigerants for a glass capillary micro cryogenic cooler," *Cryogenics* **50** (2010), pp. 439-442.

9. Lewis, R., Wang, Y., Bradley, Huber, M.L., Radebaugh, R., and Lee, Y.C., "Experimental investigation of low-pressure mixtures for micro cryogenic coolers," *Cryogenics* **54** (2013), pp. 37-43
10. Wang, Y., "Polymer-Based Micro Cryogenic Coolers," Ph.D. Thesis, Mech. Eng. Dept., University of Colorado, Boulder (2012).
11. Wang, Y., Lewis, R., Radebaugh, R., Lin, M.-H., and Lee, Y.C., "A Monolithic Polyimide Micro Cryogenic Cooler: Design, Fabrication, and Test," *J. Microelectromechanical Systems*, IEEE, Accepted for publication (2014).
12. Lewis, R., Lin, M.-H., Wang, Y., Cooper, J., Bradley, P., Radebaugh, R., Huber, M., and Lee, Y.C., "Demonstration of an Integrated Micro Cryogenic Cooler and Miniature Compressor for Cooling to 200 K," *Proc. ASME International Mech. Eng. Congress and Exposition* (2011), IMECE2011-63908.
13. Lewis, R., Wang, Y., Schneider, H., Lee, Y.C., and Radebaugh, R., "Study of Mixed Refrigerant Undergoing Pulsating Flow in Micro Coolers with Precooling," *Cryogenics* **57** (2013), 140-149.
14. Radebaugh, R., "Recent Developments in Cryocoolers," *Proc. 19th International Congress of Refrigeration*, The Hague, Netherlands, 1995, pp. 973-989.
15. Liu D., and Garimella, S. V., "Flow Boiling Heat Transfer in Microchannels," *J. Heat Transfer* **129** (2007), pp. 1321-1332.
16. [www.cryogenics.nist.gov](http://www.cryogenics.nist.gov).